Molecular Gas in the ISM

- Formation of H_2
- Molecular Gas Mass
- Properties of Molecular Clouds
- See Draine's book:
  - **Ch 5 (energy levels)**
  - **Ch 20.1, 31 (H_2)**
  - **Ch 19.3, 19.6, 32 CO**
  - Ch 33 (chemistry)
  - arXiv:1210.6990 [Scoville]
- PDR's
- Ch 16 & 31.7

Electronic, Vibrational, and Rotational Energy Levels in Molecules

Internuclear Potential

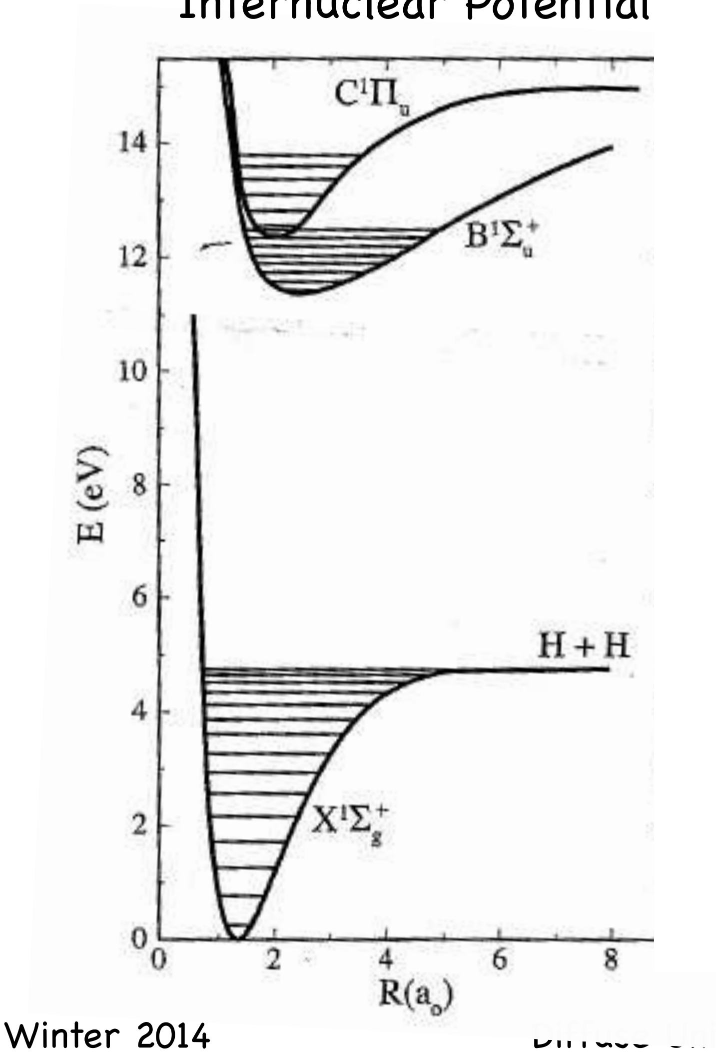

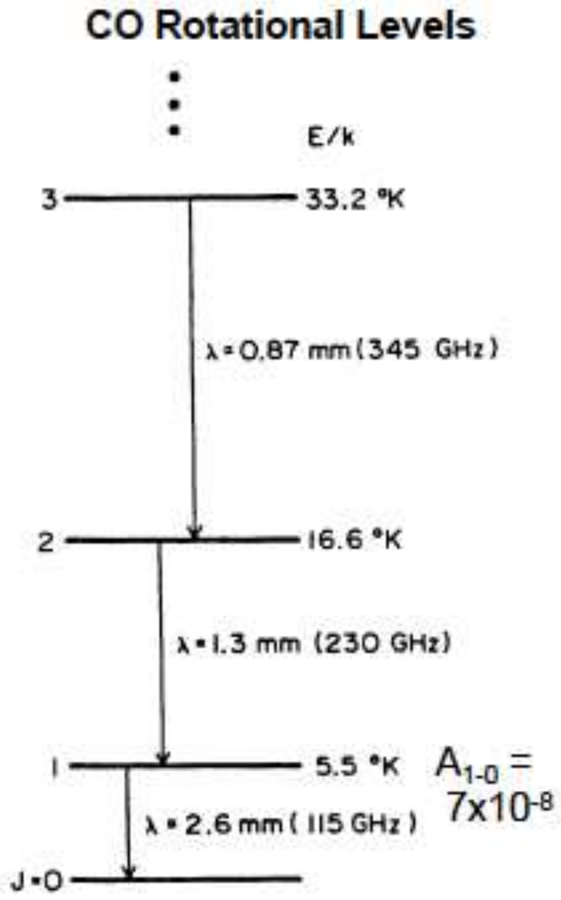

Electronic, Vibrational, and Rotational Energy Levels in Molecules

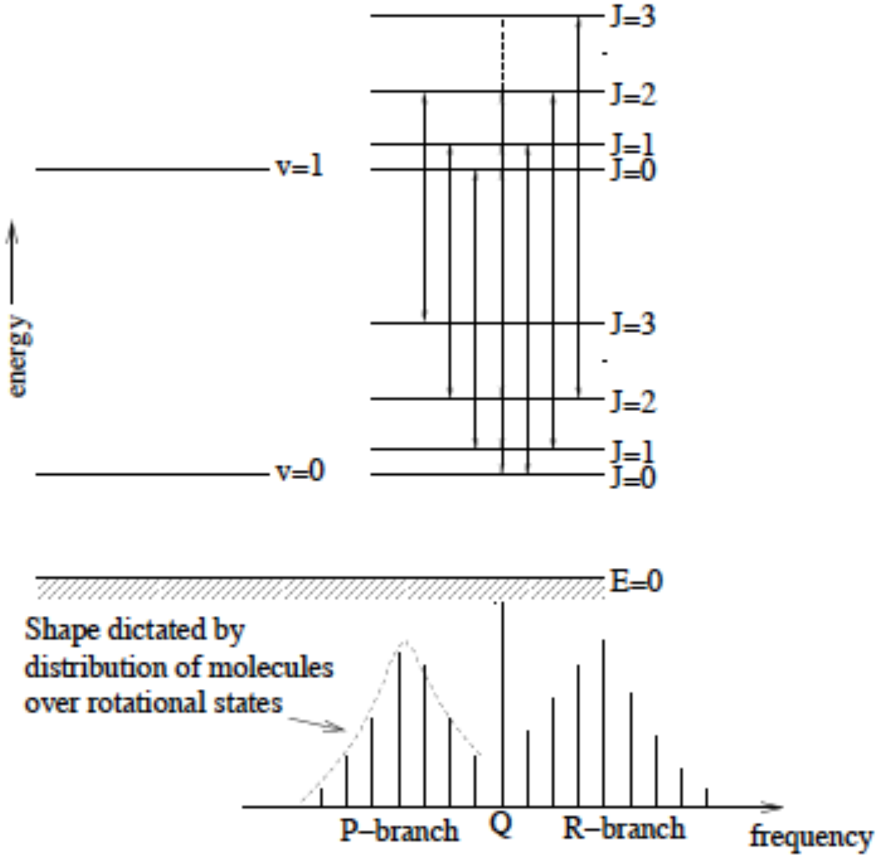

ΔJ=-1 ΔJ=0 ΔJ=+1

Molecular Gas in Galaxies

- About 22% of the ISM is in molecular clouds, where the bulk of the H atoms are in molecules.
- Nearly 100% of the H in the centers of many starburst galaxies is molecular.
- Some low metallicity (i.e., low mass) galaxies have a tiny molecular gas fraction.

Cloud Complexes and Their Components

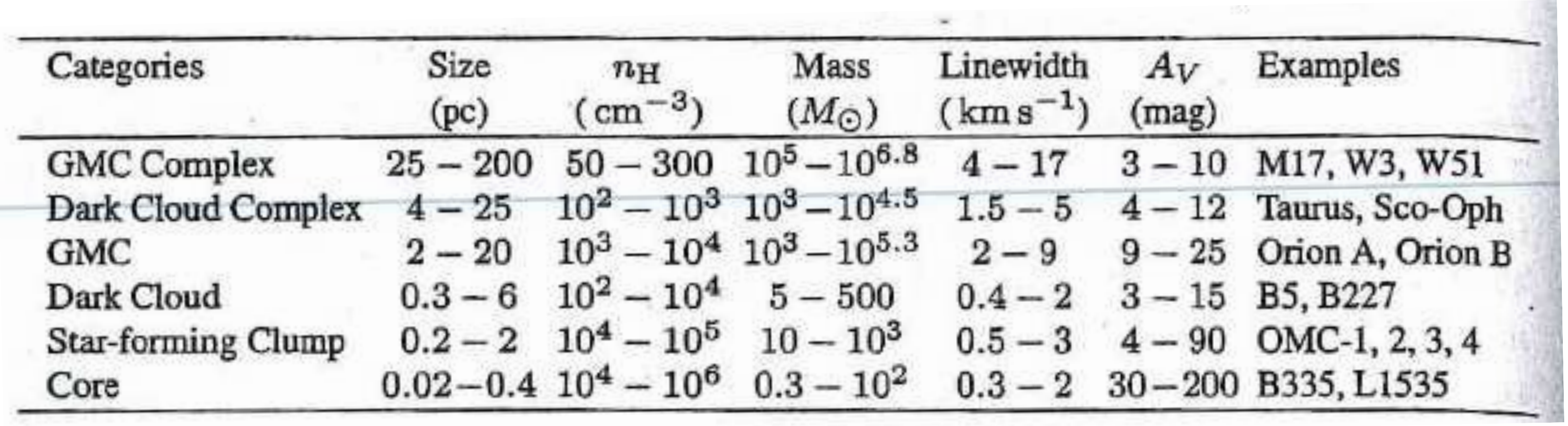

Categories	Size (pc)	n_H (cm^{-3})	Mass ($M_\odot$)	Linewidth ($km\,s^{-1}$)	A_V (mag)	Examples
GMC Complex	25 – 200	50 – 300	$10^5 - 10^{6.8}$	4 – 17	3 – 10	M17, W3, W51
Dark Cloud Complex	4 – 25	$10^2 - 10^3$	$10^3 - 10^{4.5}$	1.5 – 5	4 – 12	Taurus, Sco-Oph
GMC	2 – 20	$10^3 - 10^4$	$10^3 - 10^{5.3}$	2 – 9	9 – 25	Orion A, Orion B
Dark Cloud	0.3 – 6	$10^2 - 10^4$	5 – 500	0.4 – 2	3 – 15	B5, B227
Star-forming Clump	0.2 – 2	$10^4 - 10^5$	$10 - 10^3$	0.5 – 3	4 – 90	OMC-1, 2, 3, 4
Core	0.02–0.4	$10^4 - 10^6$	$0.3 - 10^2$	0.3 – 2	30–200	B335, L1535

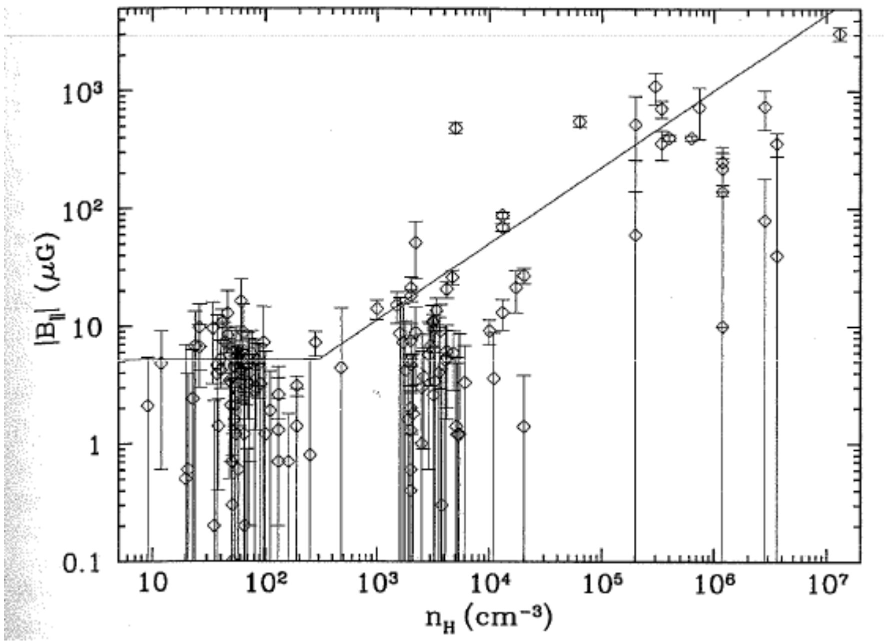

- Magnetic field strength measured from Zeeman splitting in OH, CN, HI.
- Magnetic pressure becomes increasing important in smaller, denser clouds.

Observations of Molecular Clouds

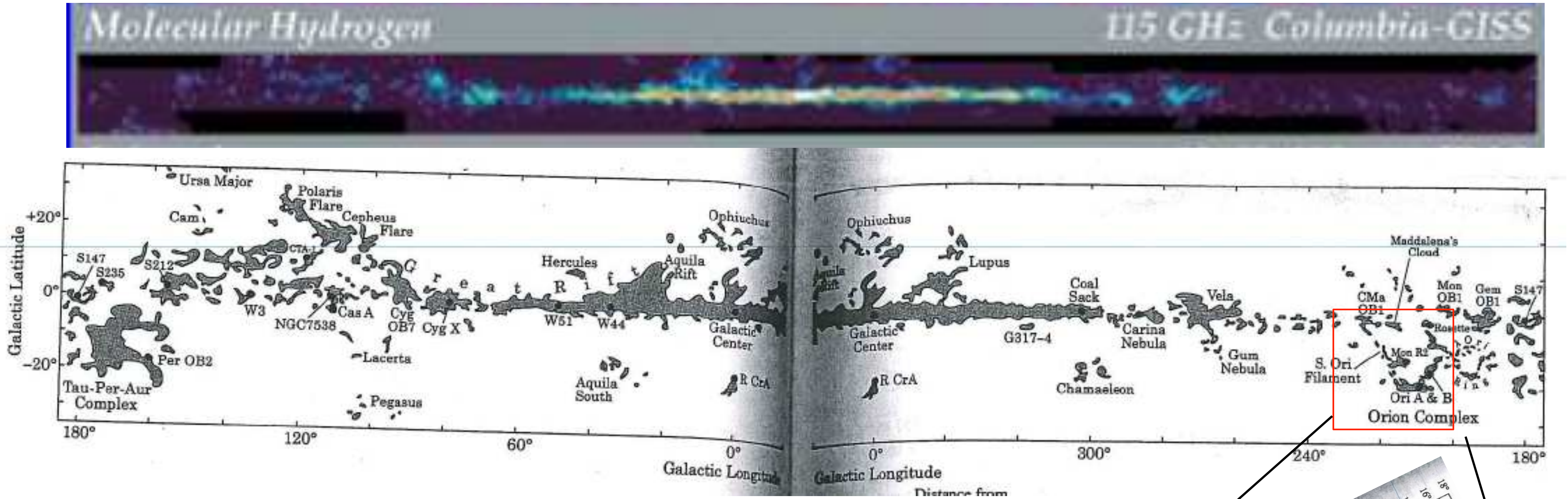

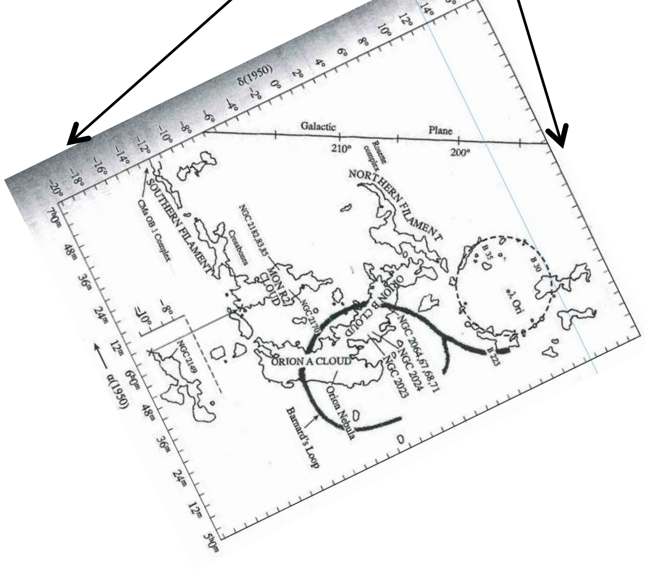

GMC Complex
(e.g., Orion, M17, W3, W51)

- 25-200 pc
- n(H) = 50 – 300 cm^{-3}
- $10^5 - 10^{6.8}\ M_O$
- A_V = 3-10 mag
- Linewidth ~ 4 – 17 km/s

Giant Molecular Cloud
(e.g., Orion A, Orion B)

- 2 – 20 pc
- n(H) = $10^3 - 10^4\ cm^{-3}$
- $10^3 - 10^{5.3}\ M_O$
- A_V = 9-25 mag
- Linewidth ~2-9 km/s

Orion Star-Forming Complex

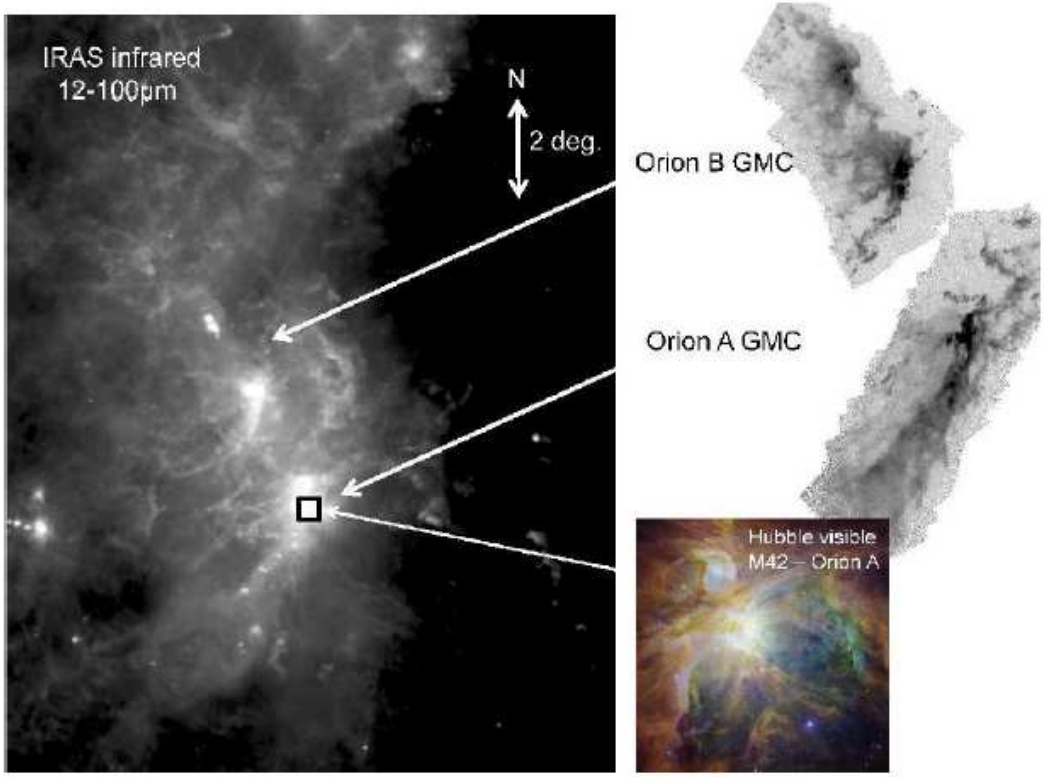

Fig. 8.3. The star-forming complex in Orion provides a close view of the complexity of both the ISM and the star formation activity. The left panel shows a very large-scale image of the FIR emission as imaged by the IR astronomical satellite (*IRAS*) (Courtesy NASA/JPL-Caltech). The upper-right panel shows the integrated CO (1–0) line emission from the two Orion GMCs (Ripple *et al.* 2012). A *Hubble* Heritage image of the visible H II region M 42 is shown at the lower right – the visible H II region occupies a very small area of the Orion complex, as outlined in the *IRAS* image.

Size-Linewidth Relation in Molecular Clouds

- $\sigma \approx 1.10$ (km/s) L^{γ}(pc), where $\gamma = 0.38$ for $0.1 < L(\mathrm{pc}) < 100$ [Larson's Law]
- More recent measurements suggest γ ~ 0.5 – 0.6
- All find σ ~ 1 km/s when L ~ 1 pc.

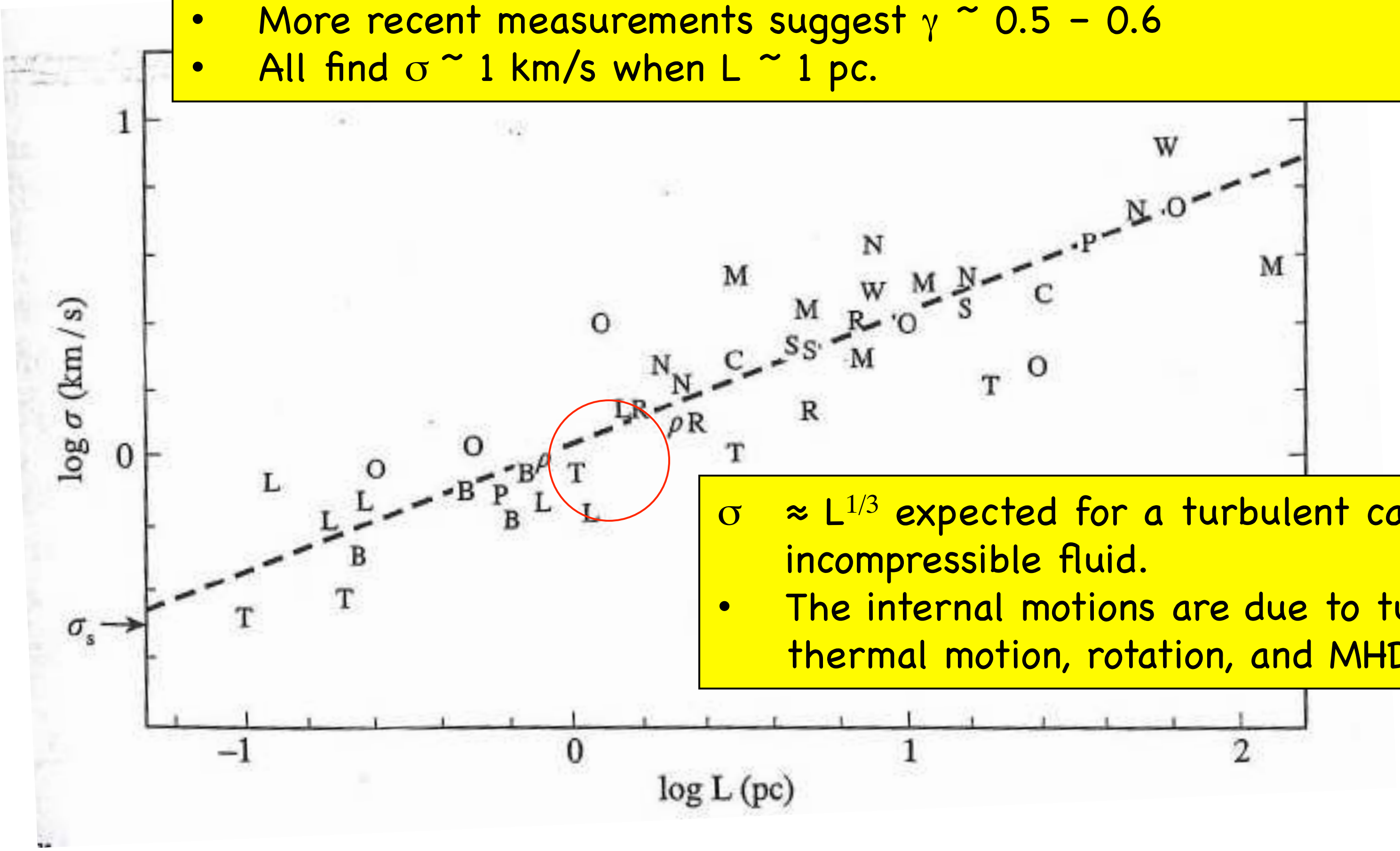

- $\sigma \approx L^{1/3}$ expected for a turbulent cascade in an incompressible fluid.
- The internal motions are due to turbulence, thermal motion, rotation, and MHD waves.

Size-Linewidth Relation for GMCs

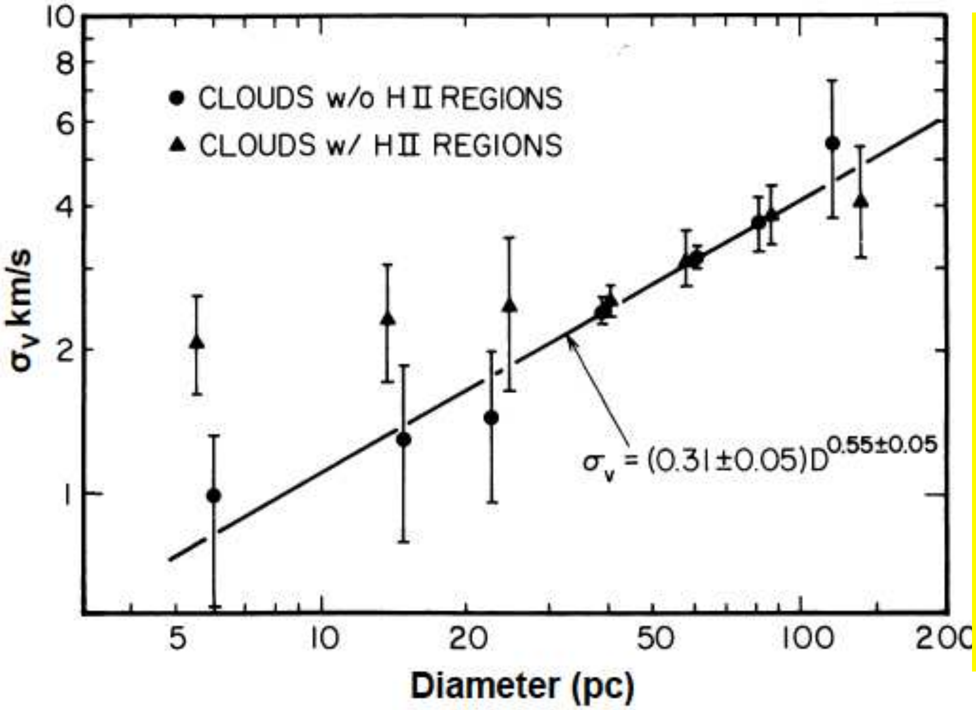

- For a D~40 pc cloud, hydrostatic equilibrium implies a mass of 4 X 10^5 M_O.
- The cloud mass distribution function is N(M) propto $M^{-1.6}$.
- D~40 pc is the scale for which half the Galactic H_2 mass is in larger/smaller clouds.

Fig. 8.4. The internal velocity dispersions of GMCs are shown as a function of diameter for clouds with and without giant HII regions, i.e., HII regions more luminous than M 42 (Scoville *et al.* 1987). This illustrates the empirical correlation found between cloud size and linewidth (the so-called size-linewidth correlation). The HII region clouds depart from this size-linewidth at low masses/sizes presumably due to feedback effects from massive star formation.

Gas Surface Density vs. Galactocentric Radius

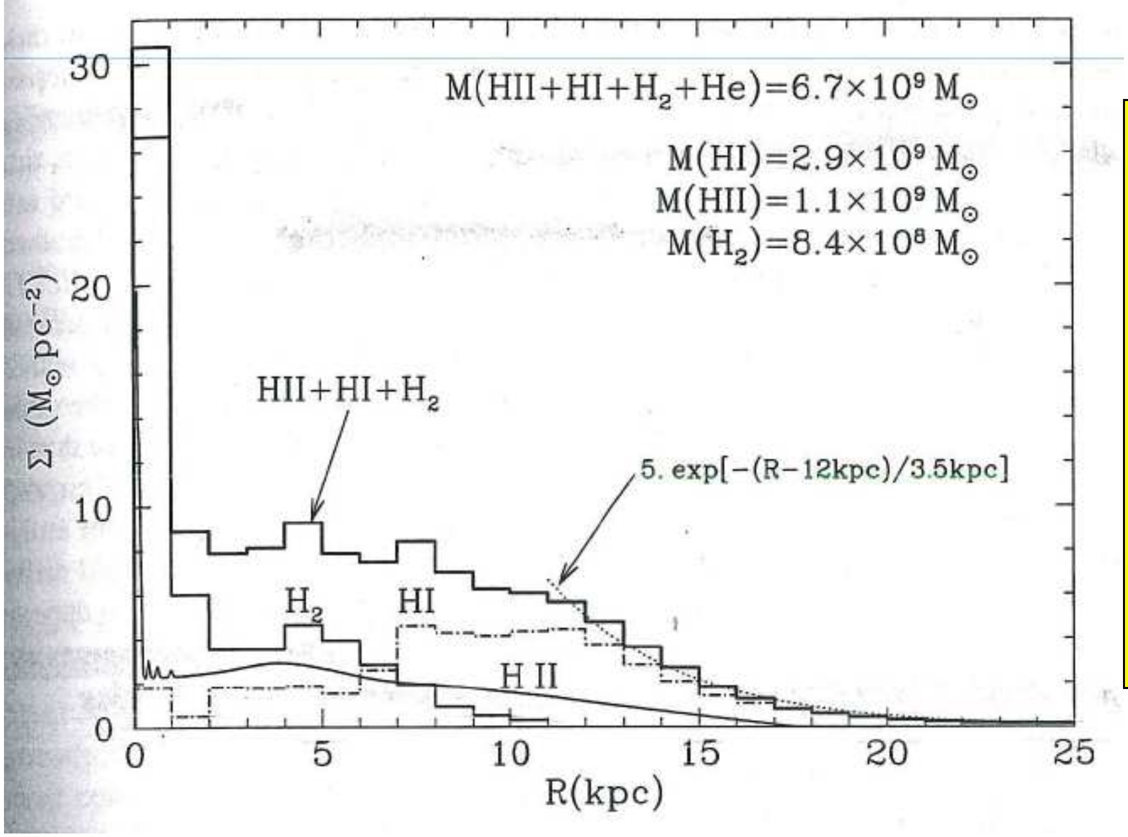

- The ISM is mostly H_2 near the center of the Milky Way.
- At RO ~ 8.5 kpc, most of the surface density is in neutral H.
- Beyond ~11 kpc, the total gas surface density declines exponentially, with a ~3.5 kpc scale length.

M51

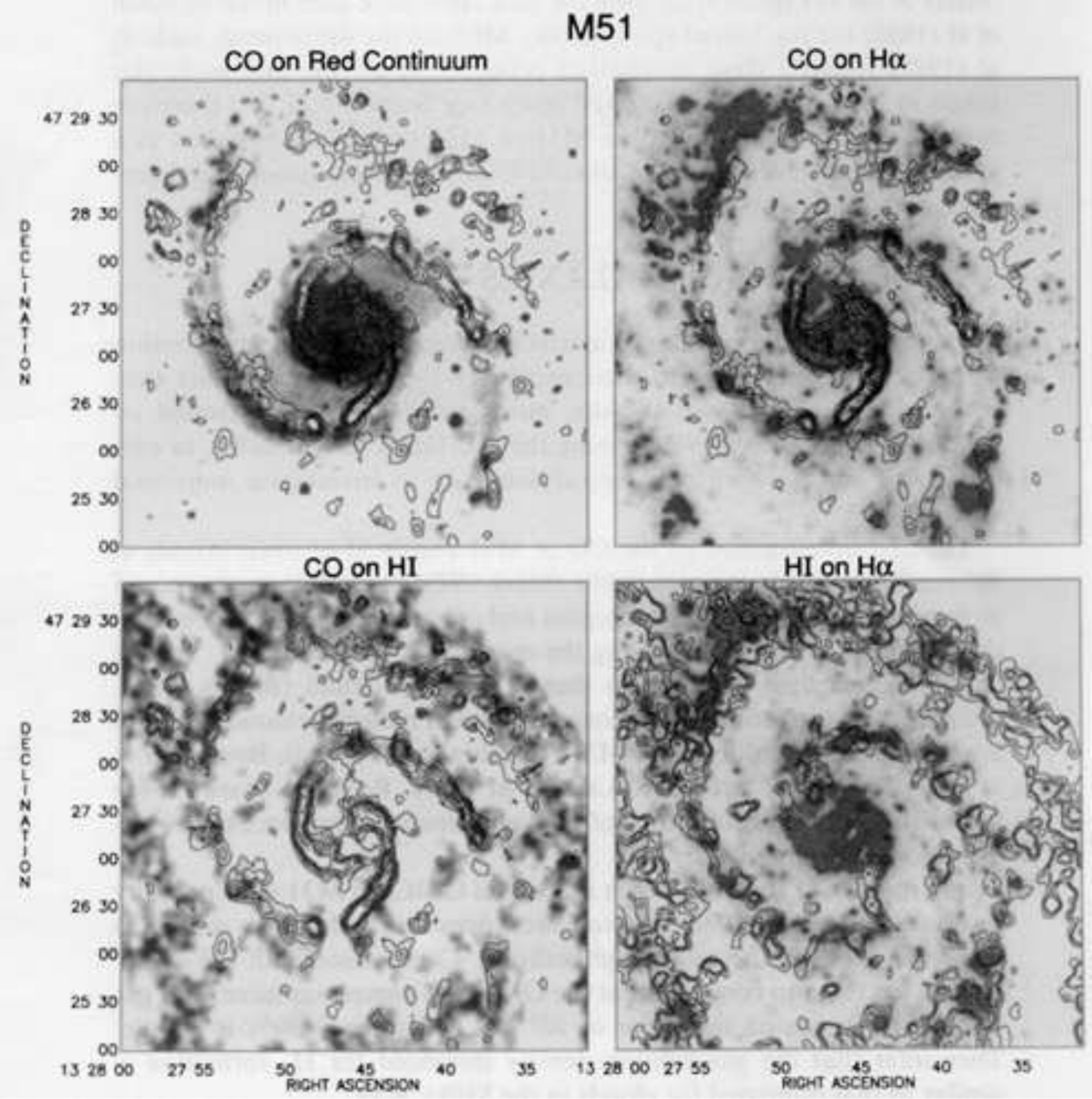
M51
CO on Red Continuum
CO on Hα
CO on HI
HI on Hα
DECLINATION
47 29 30
00
28 30
00
27 30
00
26 30
00
25 30
00
RIGHT ASCENSION
13 28 00
27 55
50
45
40
35

M83

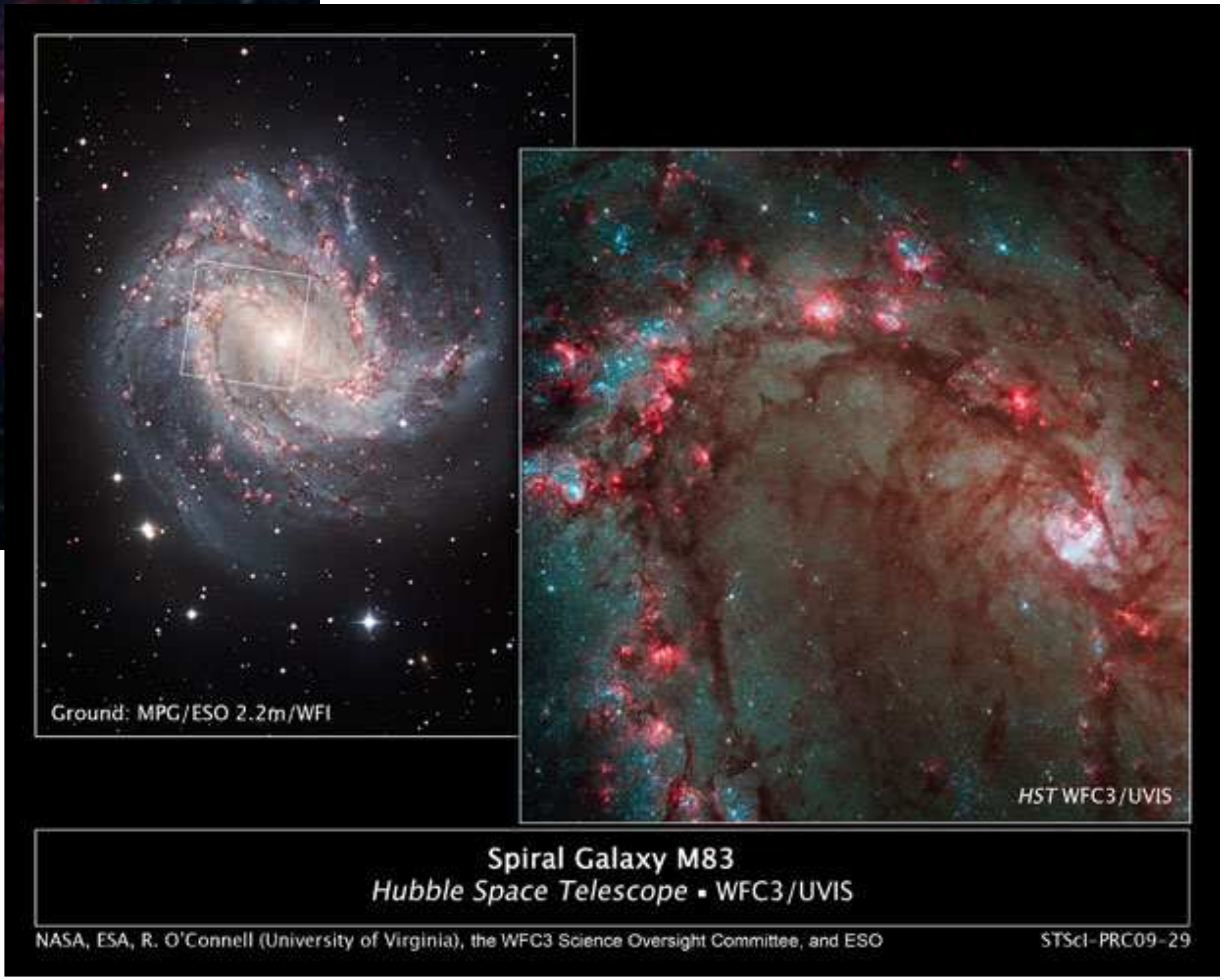

Spiral Galaxy M83
Hubble Space Telescope ▪ WFC3/UVIS

NASA, ESA, R. O'Connell (University of Virginia), the WFC3 Science Oversight Committee, and ESO

STScI-PRC09-29

Formation of H_2

- No electric dipole moment when two free H atoms approach.
- In principle, electric quadrupole radiation can remove energy from the system and leave the 2 H atoms in a bound H_2 state.
  - The rate coefficient for $H + H \rightarrow H_2 + h\nu$ is so small that this Rx can be ignored.
- Gas phase
  - In a 3-body reaction, a third H atom can carry off the energy released when H_2 is formed: $3\ H \rightarrow H_2 + H + KE$
  - These 3-body reactions are extremely slow and are only important at high densities in protostars and their disks.
  - Forms by radiative association ($H + e- \rightarrow H^- + h\nu$) and associative detachment ($H- + H \rightarrow H_2 + e- + KE$) in the absence of dust (e.g., first stars and galaxies).
  - Rate limited by density of H- which is destroyed by reactions with protons (or other positive ions) and is consequently very low.

Formation of H_2 by Grain Catalysis

- First H atom binds to grain surface. It diffuses some distance on the grain surface before it becomes trapped (i.e., thermal fluctuations at the grain temperature are unable to free it).
- When two H atoms meet in the same trap, they react to form molecular hydgrogen.
- The **4.5 eV** of energy released frees the H_2 from the grain surface.
- The measured rate coefficient (for diffuse clouds) is $R_{gr} = 3 \times 10^{-17}$ cm^3 s^{-1}, where $[dn(H_2)/dt]_{gr} = R_{gr}\, n_H\, n(H)$.
- Simple estimate in [D] 31.2 is consistent if roughly 10-50% of the grain – atom collisions produce H_2.

Destruction of H_2

- Ionization threshold for H_2 is 15.43 eV. H_2 is generally not ionized.
- Photodissociation occurs via line rather than continuum radiation.
  - $AB + h\nu \rightarrow AB^* \rightarrow A + B$
  - For H_2, photodissociation rate is ~4.2×10^{-11} s^{-1}
- H_2 absorbs over a limited range of photon energies
- Photodissociation rate depends mainly on the intensity of the radiation field in the 1100 – 912 A bandpass

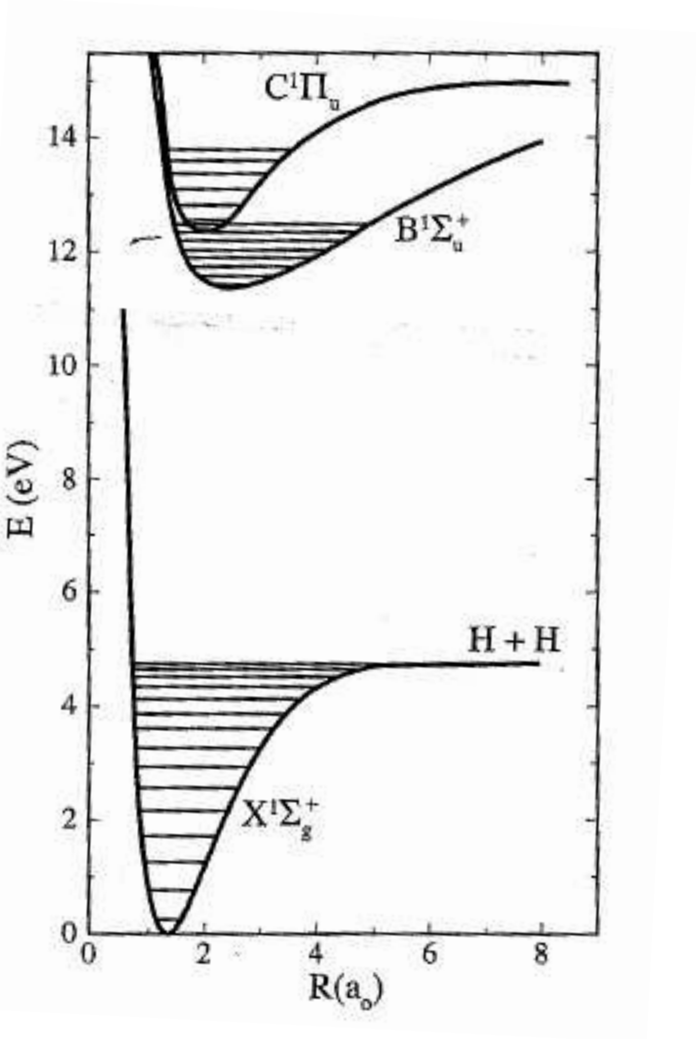

Destruction of H_2 (Cont'd)

- Inside GMCs, self-shielding reduces photodissociation rate by 3 to 5 orders of magnitude.
  - Radiative transfer calculation are required.
  - Overlap of strong H2 lines with transitions in other molecules partially shields them.
- Additional reactions include
  - Neutral-neutral exchange reactions: $AB + C \rightarrow AC + B$
  - Ion-neutral exchange reactions: $AB^+ + C \rightarrow AC^+ + B$
  - Radiative association reactions: $A + B \leftrightarrow (AB)^* \rightarrow AB + h\nu$

Electric Quadrupole H_2 Lines ($\Delta J = 2$)

Pure rotational transitions are hard to observe due to emission and absorption of the Earth's atmosphere.

J-J'	Notation	Wavelength
2-0	H_2 S(0)	28.18 um
3-1	H_2 S(1)	17.03 um
4-2	H_2 S(2)	12.28 um
5-3	H_2 S(3)	9.66 um
6-4	H_2 S(4)	8.03 um

T_K~150 K to excite J=2 by collisions.

Ro-vibrational spectrum

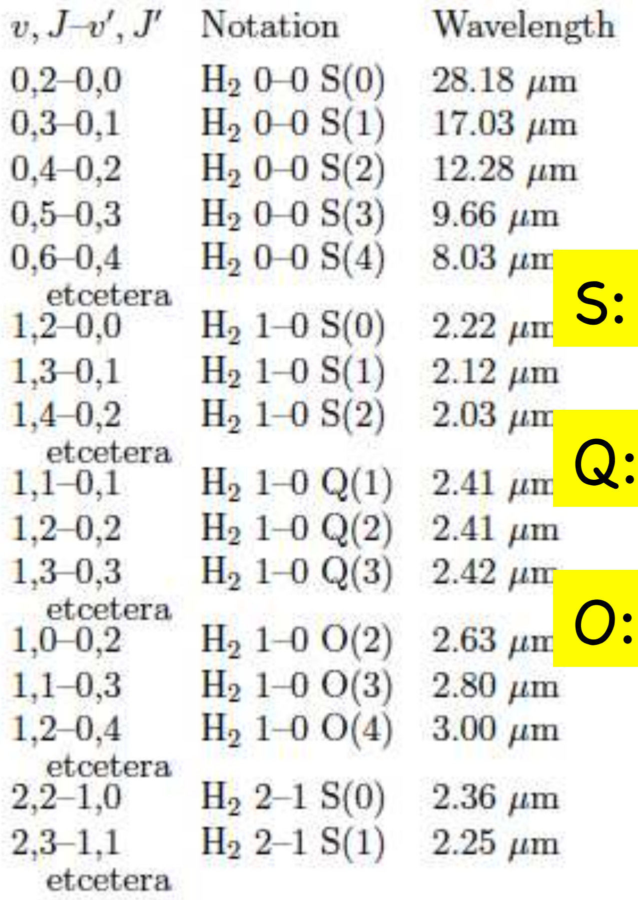

$v, J–v', J'$	Notation	Wavelength
0,2–0,0	H_2 0–0 S(0)	28.18 μm
0,3–0,1	H_2 0–0 S(1)	17.03 μm
0,4–0,2	H_2 0–0 S(2)	12.28 μm
0,5–0,3	H_2 0–0 S(3)	9.66 μm
0,6–0,4	H_2 0–0 S(4)	8.03 μm
etcetera		
1,2–0,0	H_2 1–0 S(0)	2.22 μm
1,3–0,1	H_2 1–0 S(1)	2.12 μm
1,4–0,2	H_2 1–0 S(2)	2.03 μm
etcetera		
1,1–0,1	H_2 1–0 Q(1)	2.41 μm
1,2–0,2	H_2 1–0 Q(2)	2.41 μm
1,3–0,3	H_2 1–0 Q(3)	2.42 μm
etcetera		
1,0–0,2	H_2 1–0 O(2)	2.63 μm
1,1–0,3	H_2 1–0 O(3)	2.80 μm
1,2–0,4	H_2 1–0 O(4)	3.00 μm
etcetera		
2,2–1,0	H_2 2–1 S(0)	2.36 μm
2,3–1,1	H_2 2–1 S(1)	2.25 μm
etcetera		

S: ΔJ = 2

Q: ΔJ = 0

O: ΔJ = -2

Dust Mass from FIR Emission

- At λ > 300 um, the dust emission is generally optically thin. Note that this is well into the RJ tail, so $B_\nu(T)$ propto T.
- Radiative transfer corrections are unnecessary, and the dust mass is easily measured --

$$F_\nu = (M_{DUST}/Area)\ \Omega\ \kappa_\nu B_\nu\ .$$

- The dust opacity is the absorption cross section per unit mass of dust at frequency ν. It is well measured in HI clouds but could change with composition and grain temperature.
- Example: Scoville et al. 2014 ApJ, 783, 84

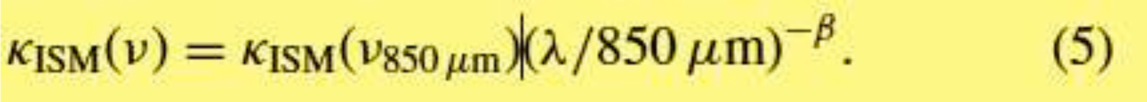

$$\kappa_{\rm ISM}(\nu) = \kappa_{\rm ISM}(\nu_{850\,\mu m})(\lambda/850\,\mu m)^{-\beta}. \qquad (5)$$

  - β = 1.8 +/- 0.1 from 7 bands of Planck data with no difference between HI and H2 regions

Dust Mass from FIR Emission

- Measured depletions of C, Mg, Si, and Fe from the gas show that HI clouds and H_2 clouds have very similar dust/gas mass ratios.
- Measuring dust mass from the RJ tail of the emission spectrum is a reasonable way to estimate the total gas mass.
- Notice that this approach does not depend on the X_{CO} factor.

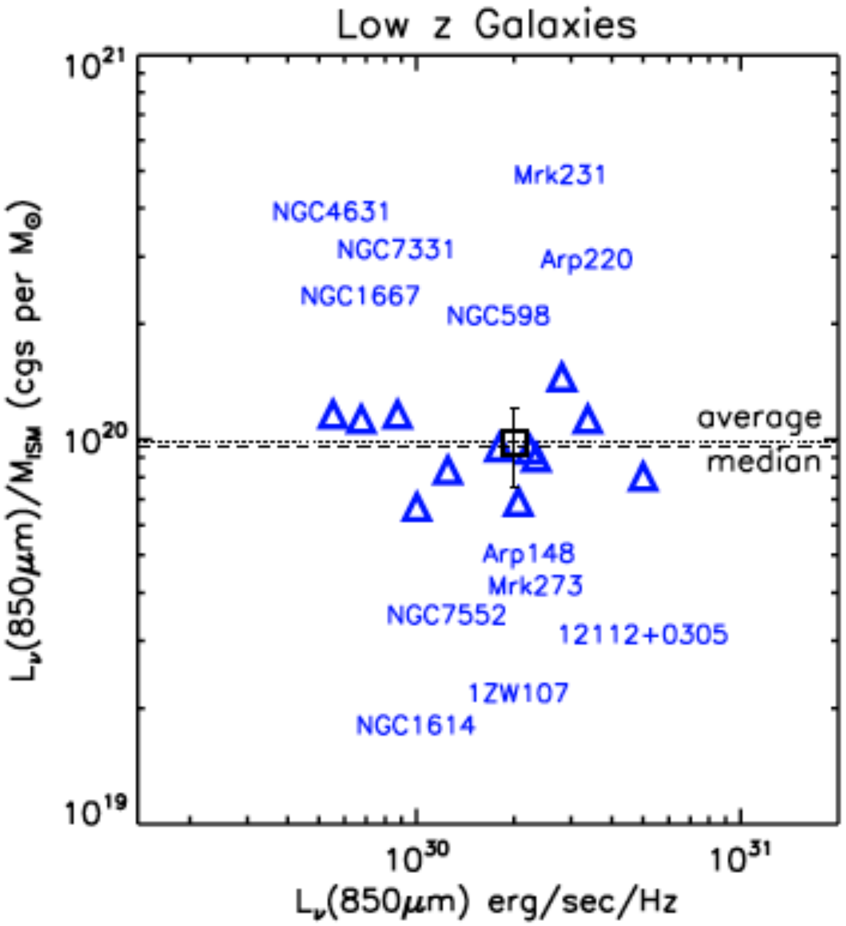

Electric Dipole Emission CO

- The rotational lines of CO are frequently used to trace molecular gas.
  - n(CO)/n(H) ≈ 7 X 10^{-5} (about 25% of the C is in CO)
  - J = 1 → 0 at ν = 115 GHZ (λ = 2.60 mm)
    - Fundamental rotation frequency = $2B_0/h$; the rotation constant, B_0 (from ch. 5), scales inversely with reduced mass.
    - A_{10} = 7 X 10^{-8} s^{-1}
  - J = 2 → 1 ν = 230 GHZ (λ = 1.30 mm)
  - J = 3 →2 ν = 345 GHZ (λ = 0.67 mm)
- Relate the CO J = 1 → 0 luminosity to H_2 mass.

The X_{CO} Factor

- Relates the CO J = 1 → 0 luminosity to H_2 mass.
- CO J = 1 → 0 is usually quite optically thick. [BB]
- At least the J = 1 level is expected to be thermalized in molecular clouds. [BB]
- How is it that the CO 1-0 emission can be used to estimate the total mass of H_2 in galaxies? [BB]

Theoretical X_{CO} Factor

- The luminosity per unit mass depends on the cloud density and the excitation temperature characterizing the population ratio n_u/n_l.
- Theoretical value of X_{CO} = $N(H_2)$ / Integral(T_A dv) excitation temperature.

The Empirical X_{CO} Factor

1. X_{CO} = 1.8 (0.3) X 10^{20} cm^{-2}/K km s^{-1}
   - Used infrared emission from dust in the Milky Way as the mass tracer (Dame + 2001)
2. X_{CO} = 1.56 (0.05) X 10^{20} cm^{-2}/K km s^{-1}
   - Used diffuse gamma ray emission to effectively count the number of H nuclei (Hunter + 1997)
   - Updated to 1.76(0.04) X 10^{20} cm^{-2}/K km s^{-1} more recently by Okumura + 2009 for Orion A GMC
3. X_{CO} ~ 4 X 10^{20} cm^{-2}/K km s^{-1}
   - Local Group galaxies (Blitz + 2007)
   - Attributed to outer layers of molecular (H_2) clouds lacking CO due to dissociation of CO. Thickness of transition layer depends on the dust abundance (and hence galaxy metallicity).
4. X_{CO} is 5 to 6 times lower in ULIRGs
   - Downes et al 1993 ApJ 414, L13

Dynamical Masses of Clouds

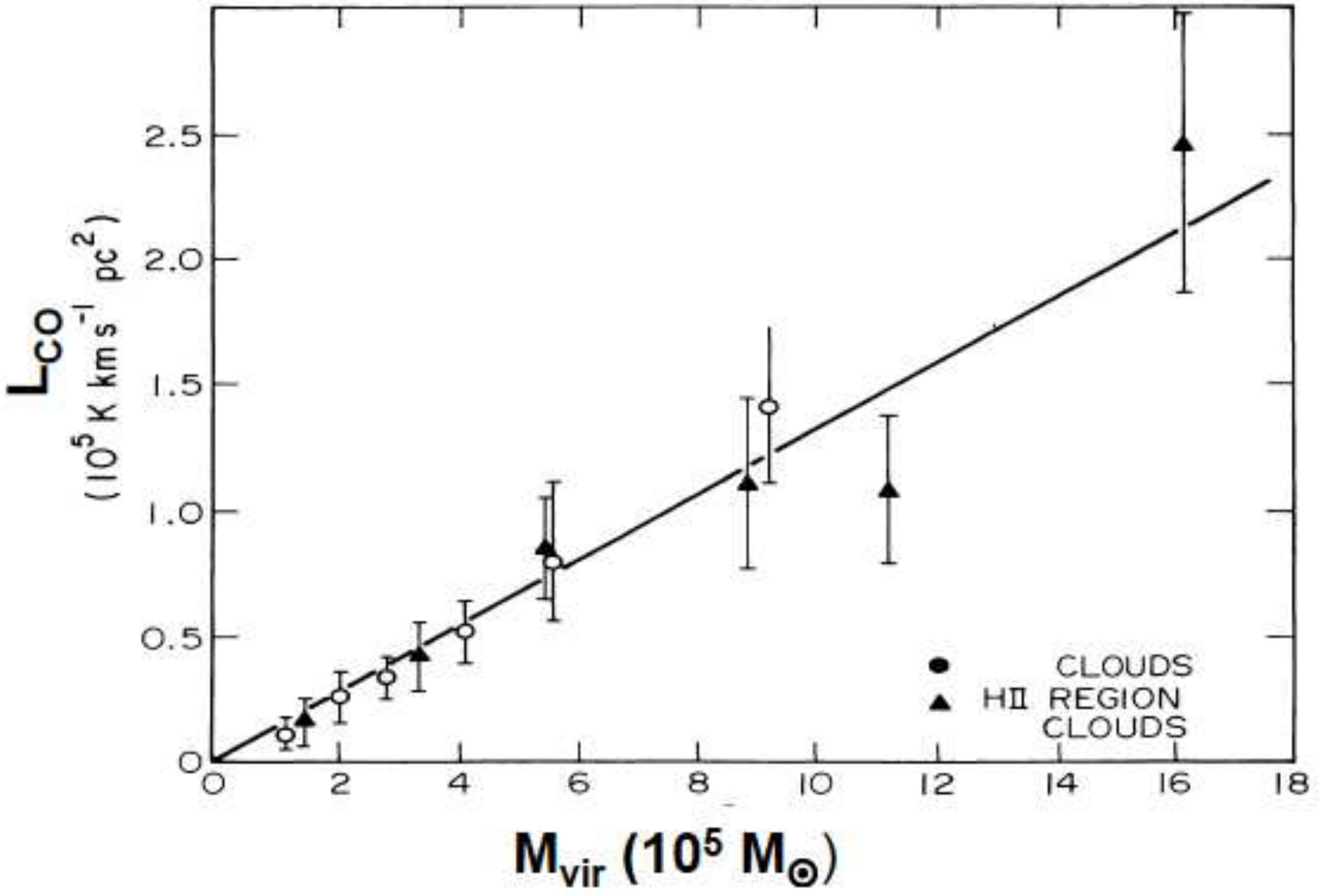

Fig. 8.5. The CO luminosities of GMCs are shown as a function of their virial masses for clouds with and without giant HII regions (Scoville *et al.* 1987).

Rotational Level Populations in H_2

- Vibrationally excited levels have radiative lifetimes of just ~10^6 s, and deexcitation by collisions with H, H_2, or He is unlikely at densities $n_H < 10^4$ cm$^{-3.}$
- The lifetimes of the lowest rotational levels in the ground vibrational state are long enough, however, that collisional effects can play a role in depopulating the lowest J levels.
- The populations of the lowest J levels are, therefore, sensitive to the H density and temperature of the gas.
  - Self-shielding affects the pumping rate of these J levels
  - To discuss the rotational excitation of H_2, we need to know
    - The UV intensity in the absence of self-shielding
    - The amount H2 between the point of interest and the UV source
    - The amount of H2 in each rotational level

Theoretical CO SLED

(Narayanan & Krumholz 2014)

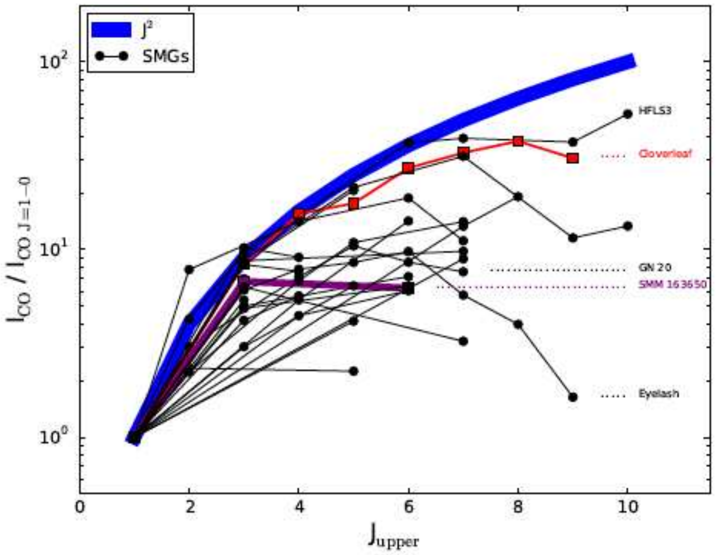

Figure 1. CO Spectral Line Energy Distributions (SLEDs) for all known high-z Submillimeter Galaxies with a CO $J = 1-0$ detection. A significant diversity in CO excitations exists, even for a given class of high-z galaxies, and it is evident that no universal line ratios are applicable. For a given line, roughly an order of magnitude uncertainty exists in the conversion ratio from high-J lines to the ground state. The blue line denotes J^2, the scaling of intensities expected if the lines are all in the Rayleigh-Jeans limit and in local thermodynamic equilibrium (LTE). The red and purple lines denote the Cloverleaf quasar and SMG SMM 163650 - two galaxies that have similar star formation rates, but starkly different SLEDs.

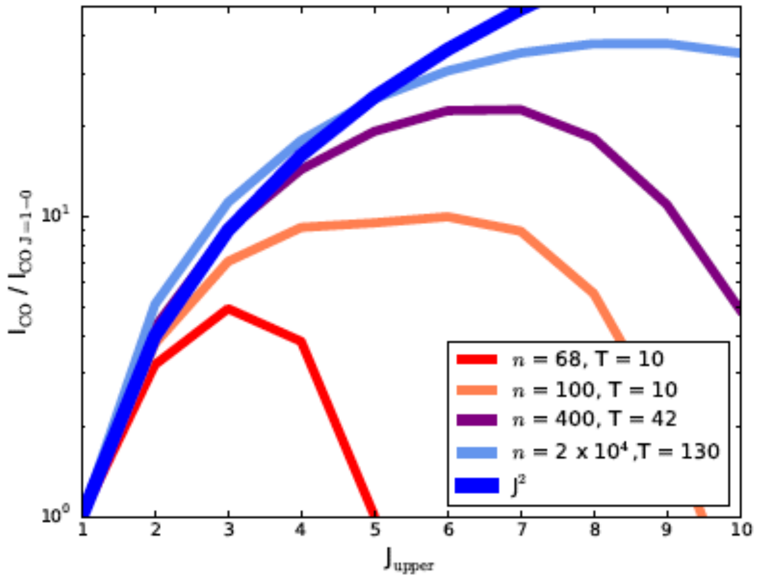

Figure 2. Model CO SLEDs for snapshots in a model galaxy merger with differing gas temperatures and densities. The blue line shows J^2 scaling, the expected scaling of intensities for levels in LTE and in the Rayleigh-Jeans limit. As densities and temperatures rise, so does the SLED. It is important to note that an individual large velocity gradient or escape probability solution with the quoted temperatures and densities may not give the same simulated SLED as shown here for our model galaxies. Our model galaxy SLEDs result from the the superposition of numerous clouds of varying density and temperature.

Rotational Excitation H_2 in Diffuse Clouds

- For low levels of self-shielding [$N(H_2) < 10^{15}$ cm^{-2}], UV pumping determines the excitation of J .GE. 2.
- The rotational distribution function fo J > 2 is relatively insensitive to the gas temperature.

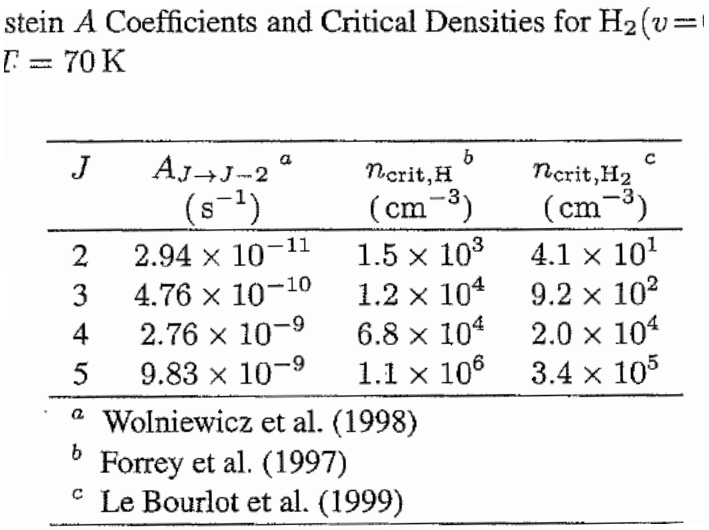

stein A Coefficients and Critical Densities for $H_2(v=$
$T = 70$ K

J	$A_{J\to J-2}$ [a] (s^{-1})	$n_{crit,H}$ [b] (cm^{-3})	n_{crit,H_2} [c] (cm^{-3})
2	2.94×10^{-11}	1.5×10^{3}	4.1×10^{1}
3	4.76×10^{-10}	1.2×10^{4}	9.2×10^{2}
4	2.76×10^{-9}	6.8×10^{4}	2.0×10^{4}
5	9.83×10^{-9}	1.1×10^{6}	3.4×10^{5}

[a] Wolniewicz et al. (1998)

[b] Forrey et al. (1997)

[c] Le Bourlot et al. (1999)

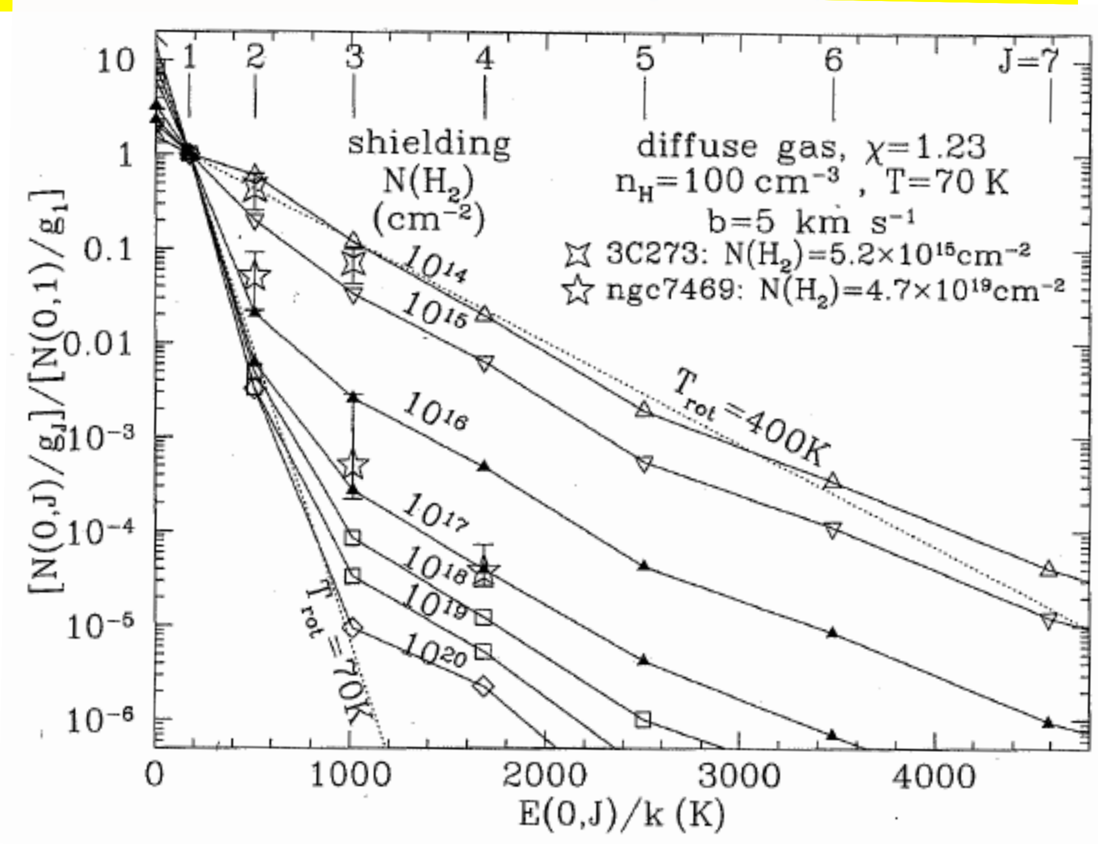

- The branching ratios in the vibration-rotation cascade determine the relative populations of the J .GE. 3 levels.
- They can be approximately characterized by rotational temperature T_{rot}~400 K indepdendently of the actual kinetic temperature.

Rotational Excitation H_2 in Diffuse Clouds

- When the shielding column increases, the UV pumping rates decline, and the fraction of H_2 in the J > 3 levels declines.
- For $N(H_2) > 10^{18}$ cm^{-2}, the UV pumping rates do no appreciably raise the population of J=2, and the relative populations of J=0 and J=2 can be used as a thermometer to estimate the gas temperature.

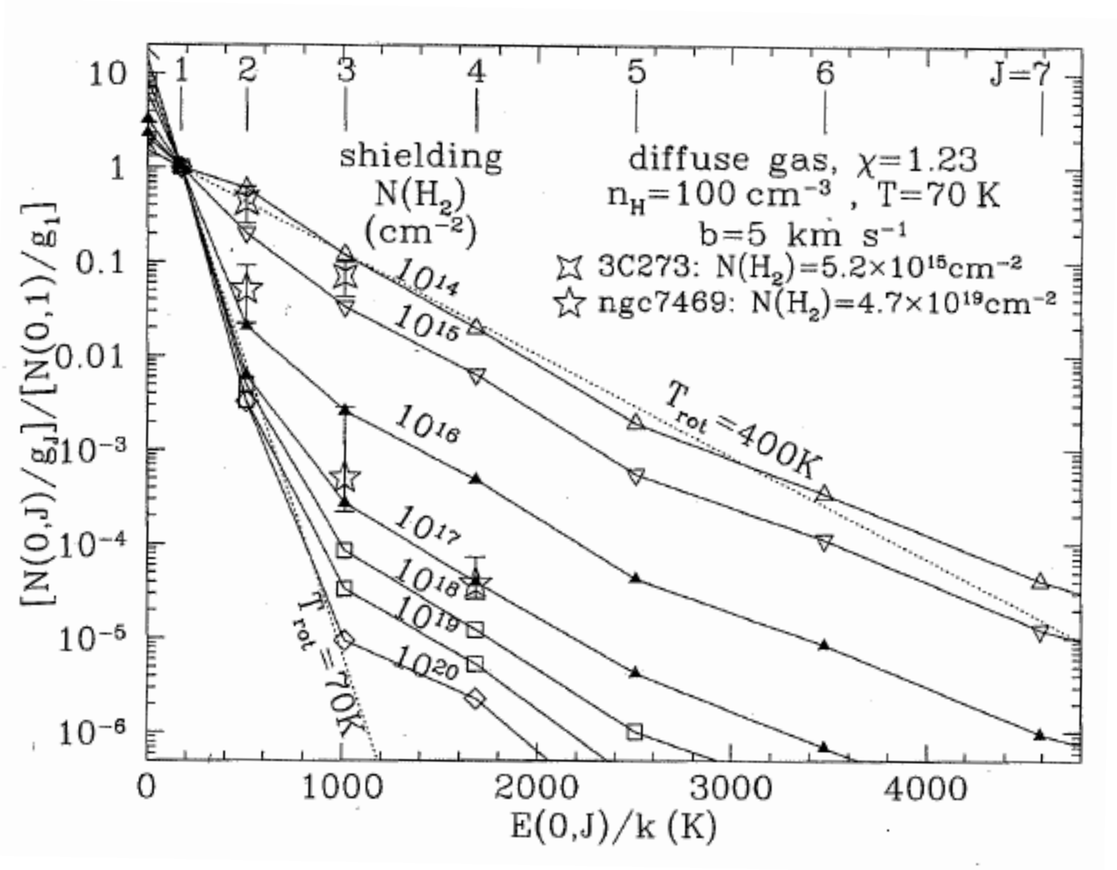

Predominantly Neutral Regions: Ionization

1. Diffuse HI regions (CNM @100K and WNM @ 5000 K)
   - Metals (e.g., C) photoionized by starlight
   - CR's slightly ionized H and He
2. Diffuse molecular cloud ($0.3 < A_V < 2$)
   - Metals still photoionized by starlight
   - CR's produce H_2^+ which leads to H_3^+
3. Dark molecular clouds ($A_V > 3$)
   - Insufficient UV radiation to photoionize metals (e.g., C and S)
   - CR's maintain $\chi = n_e / n_H \sim 10^{-7} (10^4 \text{ cm}^{-3}/n_H)^{1/2}$

Photodissociation Regions (PDRs):

The HII Region – Molecular Cloud Interface

Ionization front where the H is 50% ionized

Photodissociation front where the H is 50% atomic and 50% molecular (mass)..

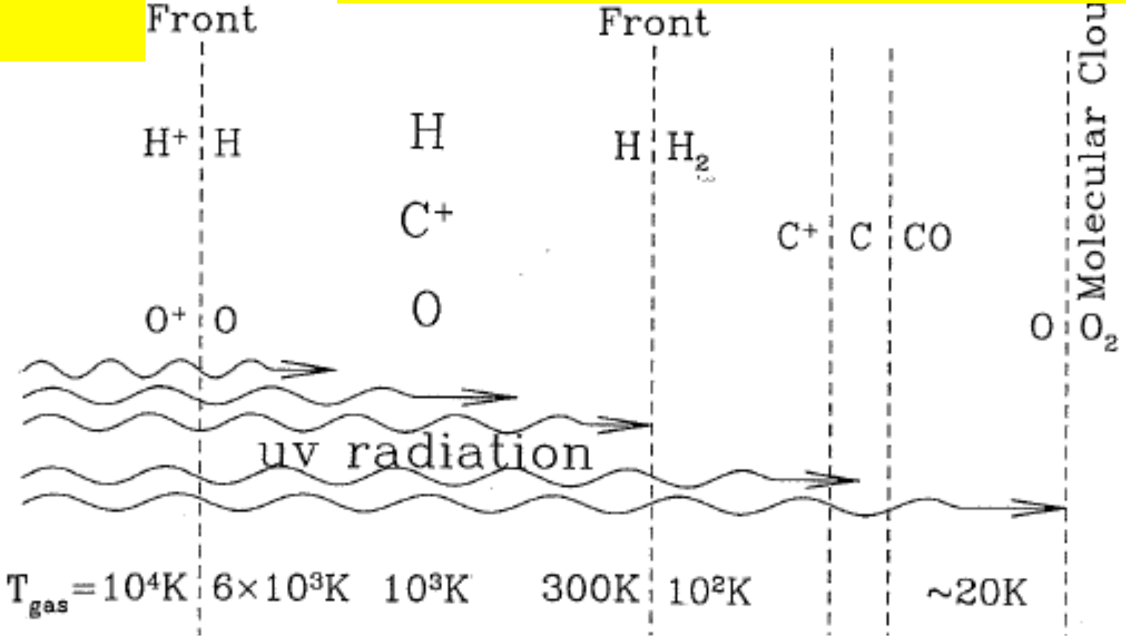

- In reference frame where PD front is at rest, the molecular gas will flow toward the PD front where it is dissociated..
- The atomic gas flows away from the photodissociation front toward the ionization front.

Photodissociation Regions (PDRs): Plane-parallel Model for Milky Way PDR

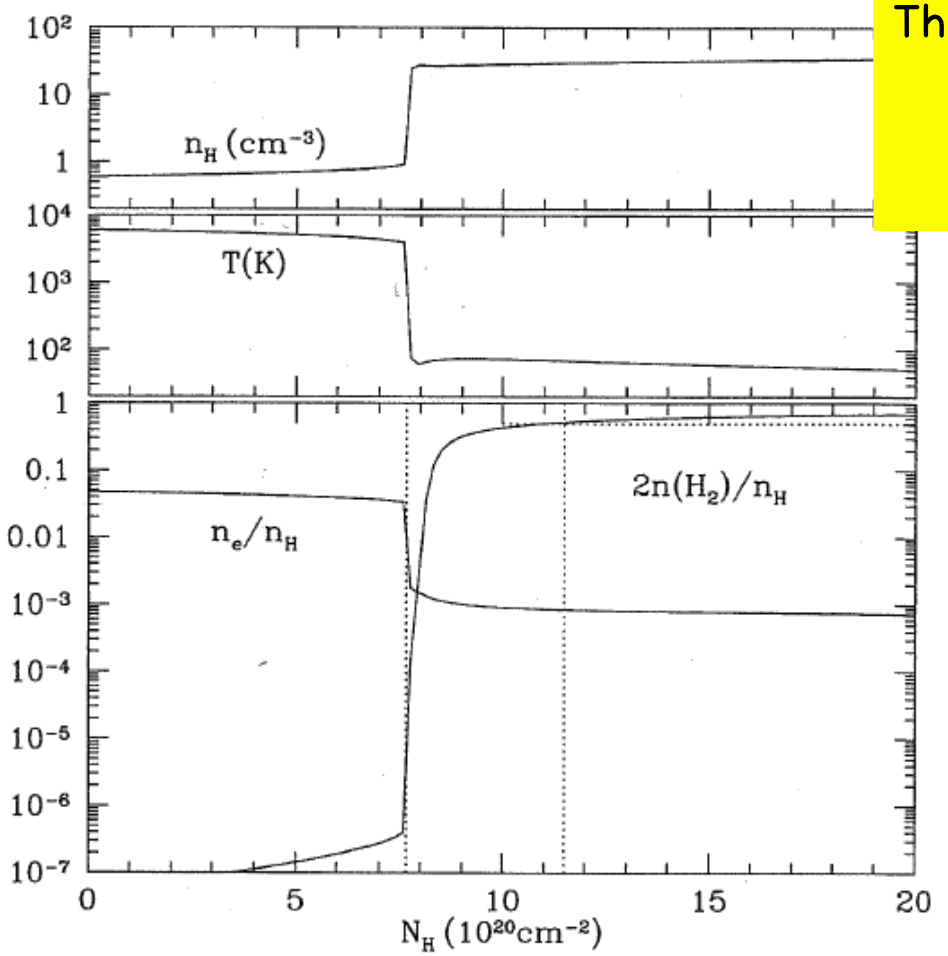

Thermal & chemical equilibrium

- Heating = cooling
- Ionization = recombination
- H2 destruction rate = formation rate

- Radiation entering the slab (from the left here) is attenuated by dust.
- The gas temperature makes a transition from the warm to the cold phase.
- The H2 abundance rises in the CNM where the self-shielding is growing.
- The radiative decay after each excitation by UV pumping results in H2 destruction 15% of the time and excitation of rotational lines 85% of the time.

Photodissociation Regions (PDRs):

UV Spectroscopy of AGN behind Diffuse Clouds

- AGN shows absorption from H_2 lines in MW
- The solid curves show the simple plane parallel slab model.

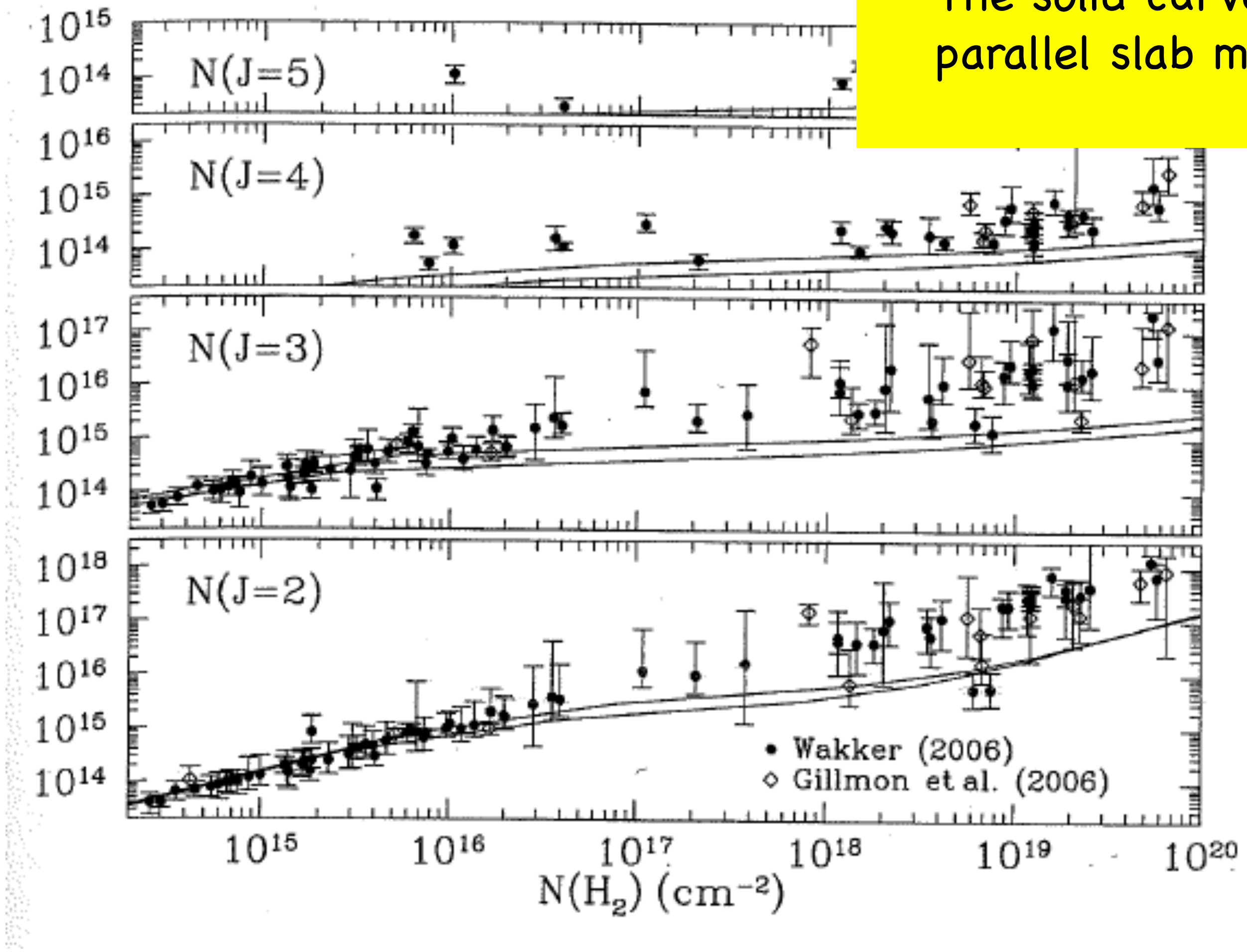

- For $N(H_2) < 10^{17}$ cm^{-2}, the model describes the observed column densities of rotationally excited H_2.
- For $N(H_2) < 10^{18}$ cm^{-2}, the model underpredicts the amount of rotationally excited molecular gas.
- Locally heated regions (turbulent decay or shocks)?

CO J=1→0 Optical Depth

* Rotation (or Excitation) Temperature:
$$\frac{n_{co}(J)}{n_{co}} = \frac{(2J+1)\, e^{-B_0 J(J+1)/kT_{ex}}}{\sum_J' (2J+1)\, e^{-B_0 J(J+1)/kT_{ex}}}$$

Rotational energy levels (5.2): $E(J) = B_0 J(J+1)$

Rotation Constant $B_0 \equiv \frac{\hbar^2}{2 m_r r_0^2}$ ← small for CO due to strong bond.

Fundamental Rotation Frequency: $\frac{2B_0}{h} = 115\ \text{GHz}$

Note $\frac{B_0}{kT_{ex}} = \frac{2.77\,\text{K}}{T_{ex}} << 1$ usually.

$$\sum_J' (2J+1)\, e^{-B_0 J(J+1)/kT_{ex}} = \underbrace{e^0}_{J=0} + \underbrace{3e^{-2B_0/kT}}_{J=1} + \underbrace{5e^{-6B_0/kT}}_{J=2} + \underbrace{7e^{-12B_0/kT}}_{J=3} + \ldots$$

= Bound between 2 functions that one can integrate.

$$\approx \sqrt{1 + \left(\frac{kT}{B_0}\right)^2}$$

* Consider a diffuse molecular cloud

$n_H \approx 10^3 n_3\ \text{cm}^{-3}$ (H nucleons)

$R = 10^{19} R_{19}\ \text{cm}$

$n(\text{CO})/n_H \approx 7 \times 10^{-5}$ (25% of C is in CO)

Gaussian velocity dispersion: $K_\nu = n_l \left(1 - \frac{n_u}{n_l}\frac{g_l}{g_u}\right) \frac{\lambda^2}{8\pi} \frac{g_u}{g_l} A_{ul} \frac{1}{\sqrt{\pi}} \frac{\lambda}{b} e^{-(\Delta v/b)^2}$

where $A_{10} = 7.16 \times 10^{-8}\ \text{s}^{-1}$

* Optical depth at line center from cloud center to cloud edge is

$$\tau_0 = K_{\nu_0} R = R\, n_l \left(1 - \frac{n_u}{n_l}\frac{g_l}{g_u}\right) \frac{\lambda^3}{8\pi^{3/2}} \frac{g_u}{g_l} \frac{A_{ul}}{b}$$

off by 3×

$$= \underset{n_H}{10^3\,\mathrm{cm}^{-3}}\,(0.260\,\mathrm{cm})^3\,\frac{1}{8\pi^{3/2}}\,\frac{7.16\times10^{-8}\,\mathrm{s}^{-1}}{2\times10^{5}\,\mathrm{cm/s}}\,10^{19}\,\mathrm{cm}\,(7\times10^{-5}) = \boxed{98.9}$$

$$\tau_0 = \boxed{297}\, n_3 R_{19}\left[\frac{n(\mathrm{CO})/n_H}{7\times10^{-5}}\right]\left[\frac{n(J=0)}{n(\mathrm{CO})}\right]\frac{2\,\mathrm{km/s}}{b}\left(1-\frac{n_u}{n_\ell}\frac{g_\ell}{g_u}\right)$$

$$\frac{n(J=0)}{n(\mathrm{CO})}\left(1-\frac{n_u}{n_\ell}\frac{g_\ell}{g_u}\right) = \frac{1}{\left[1+\left(\frac{T}{2.77\,\mathrm{K}}\right)^2\right]^{1/2}}\left(1-e^{-E_1/kT}\right)$$

$$\text{where}\quad \frac{E_1}{k} = 1(1+1)\frac{B_0}{k} = 2\,(2.77\,\mathrm{K}) = 5.54\,\mathrm{K}$$

$$\tau_0 = 297\, n_3 R_{19}\left[\frac{n(\mathrm{CO})/n_H}{7\times10^{-5}}\right]\frac{1-e^{-5.53\,\mathrm{K}/T}}{\left[1+(T/2.77\,\mathrm{K})^2\right]^{1/2}}\left(\frac{2\,\mathrm{km/s}}{b}\right)$$

Now, for a typical CO rotation temperature of $T_{ex} \approx 8\,\mathrm{K}$, we have

$$\tau_0 \approx 50\, n_3 R_{19}\left[\frac{n(\mathrm{CO})/n_H}{7\times10^{-5}}\right]\left[\frac{2\,\mathrm{km/s}}{b}\right]$$

The CO 1→0 transition is optically thick!

Critical Density for CO

- Optically Thin Case (not applicable)

$$n_{crit}\,(\text{thin}) = \frac{A_{10}}{k_{10}} = \frac{7.16 \times 10^{-8}\ s^{-1}}{6 \times 10^{-11}\ T_2^{0.2}\ cm^3\ s^{-1}} = 1200\ T_2^{-0.2}\ cm^{-3}$$

where k_{10} is the rate coefficient for collisional deexcitation of CO(J=1) by collisions with H_2.

- Optically Thick Case

+ Photons emitted near the surface have a high probability of escape, and photons emitted deep in the cloud have a negligible chance of escape.

+ Radiative Trapping [Draine 19.1 & 19.2]
The average escape probability from a homogeneous static spherical cloud is effectively the fraction of emitted photons that are emitted from a surface layer marked of ~2/3.

☆ Averaged over the line profile and the cloud volume,

$$\langle \beta \rangle_{CLOUD} \approx \frac{1}{1+0.5\tau_0}$$

$$\approx \frac{1}{1+0.5\,(50)}$$

$$\approx 0.04$$

☆ In the escape probability approximation, the rate of change of the level populations is as though the rate of spontaneous decay is only $\langle \beta \rangle A_{u\ell}$. See [D] eq. 19.7.

$$n_{crit,H_2}(CO, J=1) = \frac{\langle \beta_{10} \rangle A_{10}}{k_{10}}$$

$$= \frac{0.04\,(7.16\times10^{-8}\,s^{-1})}{6\times10^{-11}\,T_2^{0.2}}$$

$$\approx 50\,T_2^{-0.2}\,cm^{-3}$$

⇒ The J=1 level is expected to be thermalized (i.e., in LTE) in molecular clouds with

$$n_{H2} = 0.5 n_H > 50\,cm^{-3}$$

$$n_H > 100\,T_2^{-0.2}\,cm^{-3}$$

(1) See slide on thermalization of higher J levels.

19.4 (2) "Sobolev approximation" – applies where a large velocity gradient is present compared to Δv_{th}.

$$\langle \beta \rangle = \frac{1-e^{-\tau_{Sob}}}{\tau_{Sob}}$$

$$= \frac{1-e^{-K\lambda_{ul}/|dv/dr|}}{K\lambda_{ul}} \left|\frac{dv}{dr}\right|$$

... Doppler shifting of line facilitates escape.

(3) Turbulent clouds $b \to \sigma_v$

CO Luminosity of a Cloud

$$L_{ul} = \int n_u A_{ul} h\nu_{ul} \langle\beta\rangle_{cloud} \, 4\pi r^2 dr$$

$$\approx \frac{4\pi}{3} R^3 n_u A_{ul} h\nu_{ul} \frac{1}{\underbrace{1+0.5\tau_0}_{\approx 0.5\tau_0}}$$

19.30 where $\tau_0 = \frac{g_u}{g_l} \frac{A_{ul}\lambda_{ul}^3}{8\pi} \left(\frac{5}{2\pi G}\right)^{1/2} \frac{n_l R^{3/2}}{M^{1/2}} \left(1 - \frac{n_u}{n_l}\frac{g_l}{g_u}\right)$

gives us

$$L_{ul} = \frac{4\pi}{\cancel{3}} R^3 \cdot \cancel{A_{ul}} h\nu_{ul} \quad \frac{\cancel{2} \cdot \cancel{8\pi}}{\cancel{A_{ul}} \lambda_{ul}^3} \left(\frac{2\pi G}{5}\right)^{1/2} \frac{\cancel{M^{1/2}}}{\cancel{R^{3/2}}} \frac{1}{\frac{g_u}{g_l}\frac{n_l}{n_u}\left(1 - \frac{n_u}{n_l}\frac{g_l}{g_u}\right)}$$

$$= 32\pi^2 \frac{2}{3} \left(\frac{2\pi G}{5}\right)^{1/2} \frac{h\nu_{ul}}{\lambda_{ul}^3} \frac{M}{\cancel{R^3}} \frac{\cancel{R}^{3/2}}{M^{1/2}} \cancel{R^3} \frac{1}{\left(\frac{g_u n_l}{g_l n_u} - 1\right)}$$

$$\frac{L_{ul}}{M} = 32\pi^2 \frac{2}{3} \left(\frac{2\pi G}{5}\right)^{1/2} \frac{hc}{\lambda_{ul}^4} \left(\frac{\frac{4}{3}\pi R^3}{M}\right)^{1/2} \frac{1}{\left(\frac{4}{3}\pi\right)^{1/2}} \left(\frac{1}{e^{h\nu/kT}-1}\right)$$

$$\frac{L_{ul}}{M} = 32\pi^2 \left(\frac{\cancel{4}}{9_3} \frac{2}{5} \frac{\cancel{3}^1}{\cancel{4}} G\right)^{1/2} \frac{hc}{\lambda_{ul}^4} \frac{1}{\langle\rho\rangle^{1/2}} \frac{1}{e^{h\nu/kT}-1}$$

$$''\left(\frac{2G}{15}\right)^{1/2}$$

- The luminosity per unit mass depends on the cloud density ρ and on the excitation temperature T characterizing the population ratio n_u/n_l.
- The luminosity is <u>independent</u> of the actual abundance of $n(\text{CO})$ provided it is large enough that $\tau_0 >> 1$.

The CO "X – Factor"

Suppose the cloud is larger than the antenna beam. Then we can relate T_A integrated over the line to the total H column density.

$$\int T_A(1-c)\, dv \equiv \frac{\lambda^3}{2k} \int I_\nu\, d\nu$$

$$L_{u\ell} = 4\pi d_L^2 \cdot F_{u\ell} = 4\pi d_L^2 \cdot \pi\left(\frac{R}{r}\right)^2 \int I_\nu d\nu$$

$$\frac{M / 1.4 m_H}{R^2} = N_H$$

Assume $N(H_2) = 0.5 N_H$

19.34

19.35 $$X_{CO} = \frac{N(H_2)}{\int T_A\, dv} = \frac{1}{8\pi} \frac{k\lambda}{hc} \left(\frac{15}{2.8\, G m_H}\right)^{\frac{1}{2}} (n_H)^{\frac{1}{2}} \left(e^{h\nu/kT_{ex}} - 1\right)$$

$$= 1.58 \times 10^{20}\, n_3^{\frac{1}{2}} \left(e^{5.5\,K/T_{ex}} - 1\right) \frac{cm^{-2}}{K\ km/s}$$

For $T_{ex} = 8\,K$ and $n_H = 10^3\ cm^{-3}$, the prediction is

$$\boxed{X_{CO} = 1.56 \times 10^{20}\ cm^{-2} / K\ km/s}$$

+ Assumed self-gravitating clouds $\sigma_v^2 = GM/5R$

+ Doesn't count outer layers where CO is dissociated

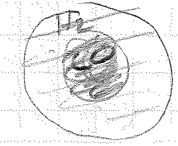

30% of mass in a Galactic Cloud.

Scoville
arXiv: 1210.6990

Molecular Masses from $\tau >> 1$ CO emission

- For a resolved cloud the integrated brightness temperature can be integrated over the projected area of the cloud to yield a line luminosity.

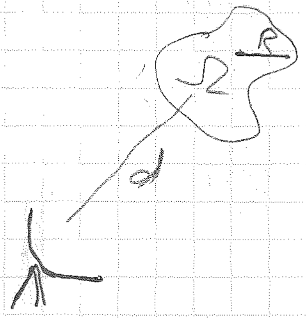

$$L_{co} = d^2 \cdot \int I_{co}\, d\Omega$$

$$\text{Area} = \Omega \cdot d^2$$

$$I_{co} = \int_{\text{line profile}} T_B \, dV$$

$$L_{co} = T_B(co) \cdot \Delta V \cdot \pi R^2 \qquad K \, \frac{km}{s} \, pc^2$$

- For clouds in virial equilibrium,

$$\Delta V = \sqrt{\frac{GM}{R}} \qquad\qquad \frac{GM}{R^2} = \frac{\Delta V^2}{R}$$

and

$$L_{co} = \pi R^2 \sqrt{\frac{GM}{R}} \; T_B \; \frac{M^{1/2}}{(\rho \frac{4}{3} \pi R^3)^{1/2}}$$

$$= \sqrt{\frac{3\pi G}{4\rho}} \; T_B \; M_{GMC}$$

$\Rightarrow$ We expect a linear scaling between cloud mass and CO luminosity provided clouds have approximately similar mean density and temperature.

Clearly, the constant of proportionality will vary as $T / \sqrt{\rho}$.

Why Does This Work?

The increased mass of larger clouds gets reflected in an increased surface area emitting CO photons and an increased linewidth over which they are emitted.

- increases in T and ρ partially compensate each other (Figure 5)

What About Extragalactic Clouds where GMCs are not Resolved?

Just summing individual clouds!

$$L_{CO} = T_B(CO)\ \Delta V \cdot \underline{\underline{\pi d^2}} \quad \mathrm{K\ km/s\ pc^2}$$

The unresolved apparent brightness temperatures vary as d^{-2}.

$$L_{CO} = \frac{A}{\Omega}\ \Omega\ \frac{T_B'}{d^2}\ \Delta V = T_B'\ \Delta V \cdot \Omega = T_B \left(\frac{GM}{R}\right)^{\frac{1}{2}} \Omega$$

$$\Rightarrow M_{H_2}(M_\odot) = \alpha_{CO}\ L_{CO} \quad \mathrm{K\ \tfrac{km}{s}\ pc^2}$$

with $\alpha_{CO} \simeq 4.9$ (Solomon & Barrett 1991)

In optically thick regions

α_{CO} should scale as CO abundance or metallicity $Z^{-0.4}$ (Scoville & Solomon 1974). The CO excitation temperature (and hence T_B) will vary as molecular abundance to the 0.4, in the photon trapping region.

ULIRGs — smoothly distributed molecular gas

CO linewidth no longer determined by self-gravity of GMCs but instead by that of stars + gas.

The linewidth will be larger than that associated with just the gas mass.

There will be more CO photons emitted per unit gas mass.

Reduces correction factor by 2-5 times in ULIGs

Downes & Solomon 1998

Bryant & Scoville 1999